IEEE Access
Multidisciplinary ⋮ Rapid Review ⋮ Open Access Journal

Received January 14, 2020, accepted January 30, 2020, date of publication February 4, 2020, date of current version February 17, 2020.

Digital Object Identifier 10.1109/ACCESS.2020.2971537

CSR-IM: Compressed Sensing Routing-Control-Method With Intelligent Migration-Mechanism Based on Sensing Cloud-Computing

ZEYU SUN[1,2], JUN LIU[1], ZHIXIAN LI[1], TIAN WANG[3,4], ZHIJIAN WANG[5], FUQIAN JIA[2], AND CHUNXIAO LAI[2]

[1]School of Computer Science and Information Engineering, Luoyang Institute of Science and Technology, Luoyang 471023, China
[2]School of Information Engineering, Henan Institute of Science and Technology, Xinxiang 453003, China
[3]College of Computer Science and Technology, Huaqiao University, Xiamen 361021, China
[4]Key Laboratories of Computer Vision and Machine Learning, Huaqiao University, Xiamen 361021, China
[5]School of Information Science, Guangdong University of Finance and Economic, Guangzhou 510320, China

Corresponding author: Zhijian Wang (zjian@gdufe.edu.cn)

This work was supported in part by the National Natural Science Foundation of China under Grant U1604149, in part by the Henan Province Education Department Cultivation Young Key Teachers in University under Grant 2016GGJS-158, in part by the Luoyang Institute of Science and Technology High-Level Research Start Foundation under Grant 2017BZ07, in part by the Key Science and Technology Program of Henan Province under Grant 192102210116 and Grant 192102210249, in part by the Henan Province Education Department Natural Science Foundation under Grant 19A120009 and Grant 20A520027, and in part by the Major Project of Basic and Applied Research in Guangdong Universities under Grant 2017WZDXM012.

ABSTRACT Considering the event-based WSNs routing, the frequent changes of topology may result to the large energy costs in the whole network. Therefore, this paper proposes a Compressed Sensing Routing-control-method with Intelligent Migration-mechanism based on Sensing Cloud-computing (CSR-IM). First, the method gives a determining the moving speed and position of the target node through compressed sensing theory, and at the same time, it gives the lower bound calculation process of the target node state estimation value at $k+1$ time by the probability knowledge. Second, with the purpose of reducing the network load, the routing tree with the center of fog nodes is established to obtain the data in the route effectively and optimize the data aggregation routing process, and then energy cost of the whole network is balanced. Finally, the simulation experiments show that method of this paper (CSR-IM) and other algorithms have improved the average data aggregation rate by 8.19%, and the average network coverage has increased by 12.65%, which proves that the proposed algorithm is effective and practical.

INDEX TERMS Intelligent migration-mechanism, sensing cloud-computing, routing-control-method, compressed sensing.

I. INTRODUCTION

As an important support for the Internet of Things (IoT), Wireless Sensor Networks (WSNs) has become a new research hotspot in the fields of wireless networks [1]–[5]. With the development of microelectronics technology, embedded low-power technology, wireless communication and data compression, WSNs have the characteristics of miniaturization, low cost, low energy consumption and distribution and can provide people with anytime, fine-grained, diversified monitoring information which has huge application potential in the fields of battlefield reconnaissance, biological habitat environmental monitoring, precision agriculture and medical monitoring [6]–[9]. WSNs are a new type of network that realizes the collection, processing, and transmission of relevant sensory data in the layout area. It usually consists of a large number of sensory nodes and sink nodes [10]–[13]. Each sensory node is self-organized and multi-hop. The sensor data is sent and relayed to the Sink in a simple manner, and the external network can obtain the real-time sensing information of each node in the sensing area through the Sink. The main function of the WSNs is to collect relevant sensing information in the layout area. Because the network monitoring area is wide and most of

The associate editor coordinating the review of this manuscript and approving it for publication was Songwen Pei.

them are deployed in the wild, each node in the network is equipped with independent power source with limited power [14]–[18]. In order to ensure the network's working life, the energy consumption of network nodes has become a key factor restricting on the performance of sensor networks. In the traditional collection processes for WSNs data, nodes need to forward data packets of other node in addition to send their own data packets. Therefore, the closer the node is to the sink, the more energy it consumes, and it is easy to exhaust its own energy in advance, which will cause the problem of ''energy Hole''; In addition, due to the dense deployment of sensor network nodes, there is a large spatial correlation of sensory data between the adjacent nodes, and there is also a large time correlation of the periodic sensory data for each node. And then, WSNs sensing data have a lot of redundancy in time and space, and there is a large compressible space. In order to extend the working life of WSNs and achieve efficient data collection, it is urgent to study new data collection strategies so that it can not only guarantee the energy balance of the network, avoid ''energy holes'', but also reduce the data redundancy in the network and reduce energy consumption in network [19].

Collecting sensory data is the main task for WSNs, and it is the basis for realizing various applications in WSNs. Data collection methods for WSNs can be divided into three categories: time-driven, query-driven, and event- driven. For data collection way of time-driven, the sensor nodes periodically sense the environment and transmit the sensed data to the base station at a fixed data rate according to pre-scheduling. This method of data collection is also called periodic data collection and is suitable for applications that require global monitoring. For data collection way of query-driven, the base station sends a data collection request according to the user's needs, and only the sensor nodes that satisfy the request send its sensing data. For data collection way of event-driven, any sensor node remains silent until the target event occurs, and the nodes that only need to monitor the events sends event-related data to the base station. These are usually sent by a part of nodes, and the randomness of the event causes that the distribution is also random [20], [21]. In order to cope with problems such as node failure and inaccurate sensing data caused by the environment, WSNs usually deploy sensor nodes densely in the monitoring area, but this also results in greater information redundancy in the whole network. If the base station collects all the original data directly, a lot of precious energy will be wasted on the transmission of redundant data. In view of this problem, data aggregation technology uses various methods to process the sensed data and reduce the redundant data transmission in the network. It is an important technology to achieve energy- efficient data collection in WSNs.

II. RELATED WORKS

With the emergence of distributed compressed sensing theory, more and more researchers have begun to pay attention to the applications of compressed sensing technology to WSNs. Paper [22] pointed out that distributed compressed sensing has good fault tolerance and security in WSNs. The advantages of high performance and adaptive channel capacity have laid the foundation for the applications of compressed sensing theory in WSNs.

The current researches on the application of compressive sensing in WSNs are mainly divided into the following five aspects:

(1) the application of data fusion in WSNs; paper in [23] proposed the use of compressive sensing combined with the spatiotemporal correlation of data Fusion of intra-network data in a way that greatly reduces intra- network communication and prolongs network life. Paper [24] proposed a hierarchical data fusion scheme based on the compression domain. The parent collection clusters at each level compress and fuse the data from lower-level clusters. The data is sent to the upper layer in turn until it reaches the top cluster head node. This solution greatly reduces the redundant data in the network, reduces the amount of data transmitted in the network, and reduces energy consumption.

(2) Application in target localization. Paper [25] adopts the iterative backtracking CS algorithm to solve the grid-based multi-target node localization problem, which can realize the simultaneous localization of multiple targets and improve the positioning accuracy. Paper [26] proposed a localization algorithm based on CS for dynamic target positioning problem. By matching the target motion law and sparse basis, the dynamic target positioning problem was transformed into a reconstruction problem for sparse signals. And the positioning performance had been improved.

(3) Application in distributed data storage by the fields of data security of WSNs. Paper [27] combined compressed sensing and network coding, and proposed a data storage scheme for compressed network coding based on space-time correlation, respectively. The method of compressing data from a time and space perspective reduced the amount of data on the network and extended the life of the network.

(4) Application in recovering lost data in sensor networks. Paper [28] used the time and space correlation and compressed sensing technology and designed a packet loss recovery algorithm for spatiotemporal data based on compressed sensing. And the proposed algorithm had great advantages than the traditional packet loss recovery algorithms such as data interpolation.

(5) Application in network data collection; this field mainly studies how to effectively implement data collection, match observation matrix and data collection routing, and minimize the amount of data transmission in the network. Paper [29] pointed out that if there is a small amount of Gaussian independent random loss of node data in the entire network, the CS reconstruction algorithm can use the correlation among the data to reconstruct the lost information, and the actual reasons for the packet loss in WSN link are complex, and It cannot be simply described by a Gaussian independent random packet loss model.

Paper [30] proposed A Distributed and Morphological Operation-based Data Collection Algorithm (DMOA), which pointed out that there is a strong time correlation among sensor data, and also proposed a joint optimization algorithm combining CS and spatio-temporal correlation to recover lost node data, but the algorithm is only applicable for the lost data recovery of the sink database, and it does not consider the problem of packet loss recovery during data collection. Paper [31] proposed the A Trust-Based Secure Routing (TBSR) algorithm, in which, some nodes are selected randomly in each round to participate in data collection. On the Sink side, an extremely sparse observation matrix is constructed based on the received node number and the entire network's original data is reconstructed. Although the method is aimed at solving the problem of CS data collection under unreliable links, it is not applicable to environments with weak spatial correlation of data on the entire network due to the extremely sparse assumption. In addition, the algorithm still uses traditional data collection methods in collecting node data, which may cause an imbalanced energy consumption problem in which the energy consumption of nodes near Sink will be exhausted in advance. Paper [32] proposed a Mobile Data Collectors (MDCS) algorithm, which used the greedy algorithm to generate a chain with the shortest distance among adjacent nodes according to the node position. The head node in the chain was in turn responsible for transmitting the aggregated data to base station. At the same time, the nodes are organized into a two-layer chain structure, i.e., multiple fixed-length low-level chains and a high-level chain composed of low-level chain heads. Data was transmitted and aggregated along the low-level chain to the high-level chain, and finally reached the base station.

Paper [33] introduced a distance threshold to avoid the generation of long chains, and selected nodes with more residual energy and closer to the base station as the chain head to balance nodes energy consumption. Paper [34] divided the network area into multiple concentric rings, and the nodes in each ring were stored to the link list. The data was first sent to the chain head, and then was sent from the outside to the base station along the chain head. Paper [35], the monitoring area was divided into rectangular horizontal sub-areas with the same size, and nodes within the same sub-area used a greedy algorithm to form a routing chain. Similar to literature [35], Paper [36] also divided the network area into rectangular sub-areas, but the algorithm divided the network area along the vertical direction, and each sub-area used a uniform step algorithm instead of a greedy algorithm to form a routing chain. Paper [37] used BeamStar technology to divide the area into several fan-shaped sub-areas, and then used the data integration control algorithm to establish a short chain, and all chain heads were built into a routing chain which was connected to the base station. Paper [38] proposed a local chain construction strategy based on Voronoi region division, which could build a routing chain with low energy consumption and less interference. Paper [39] calculated the transmission cost based on the optimal transmission power. After establishing a minimum cost tree, a distributed depth-first search was used to construct a routing chain that starts at the base station. Paper [40] first used Strip Tree Geometry algorithm to obtain a hierarchical tree, and then used an in-order traversal search based on the tree to obtain a routing chain containing all nodes. Paper [41] proposed a set of routing chain construction algorithms based on minimum spanning tree (MST). It first built an undirected MST, then used the node closest to the center of the network as the root to obtain a directed MST by breadth-first search, and finally used the first order, middle order, and post order to traverse to obtain the routing chain containing the entire network of nodes. Paper [42] divided the area into a grid. The node with the most remaining energy in each cell acted as the head. All heads form a routing chain and the head with the most remaining energy was the routing chain head.

The above studies can complete the process of data aggregation and routing selection, but in multi-hop routing, the nodes within one hop of the base station are responsible for forwarding the data of all other nodes in the network. The load is heavy and energy consumption is fast. And the density is large. Therefore, the sensed data in the network has a large redundancy. It is often necessary to perform related processing to reduce the redundancy and reduce unnecessary data transmission in the network. In event-driven WSNs, clustering of event domain nodes can easily implement de-redundant processing of event data, and establishing a suitable routing tree based on event clusters can further reduce data transmission energy consumption. Therefore, how to building a reasonable hybrid routing structure is very effective for energy saving of event-driven WSNs.

III. NETWORK MODEL AND SOLUTION

A. MODEL ESTABLISHMENT AND ANALYSIS

In order to facilitate the research, we make the following assumptions about the WSNs:

1. In the initial phase, all sensor nodes have equal energy and are isomorphic [43]–[45].

2. The sensing areas of all sensor nodes are discs and their own position information can be obtained by the positioning algorithm (e.g. RSSI, TDOA) [46], [47].

3. The migration probability and communication capability of fog nodes are higher than other sensor nodes.

4. The working hours of all sensor nodes change periodically and are synchronized on time.

Definition 1: The intersection of the sensor node coverage area and the monitoring area is called the effective coverage area.

$$\Omega_1 = \text{area}(\cup S_i) \cap \text{area}(\Omega) \tag{1}$$

where S_i represents the coverage area of any sensor node, area(Ω) represents the area of the monitoring area and Ω_1 represents the effective coverage area.

Definition 2: The ratio of the effective coverage area with the area of the monitoring area is called the effective

coverage ratio.

$$P = [\text{area}(\cup S_i) \cap \text{area}(\Omega)] \Big/ \text{area}(\Omega) \tag{2}$$

where P is expressed as effective coverage.

Definition 3: The sum of network runtimes is called the network life cycle.

Definition 4: The Euler distance between any two sensor nodes is less than the sum of the sensing radius of the sensing nodes, which are called neighbor nodes. The node set formed by neighbor nodes is called the neighbor set.

$$d(i, j) \leq R_i + R_j \tag{3}$$

where $d(i, j)$ is the Euler distance of any two sensor nodes, R_i and R_j are the sensing radius of the sensor nodes.

Definition 5: If there exists a constant $\delta_k \in [0, 1]$, and then for any sparse signal s with sparseness k has the following condition.

$$(1 - \delta_k) \|s\|^2 \leq \|\Theta s\|^2 \leq (1 + \delta_k) \|s\|^2 \tag{4}$$

It is said that the matrix Θ satisfies the RIP condition of the k-th order Restricted Isometry Property (RIP), where δ_k is called the RIP constant of the matrix Θ. Although theoretically, the sensor matrix Θ satisfies the RIP condition and can reconstruct the original signal with a high probability, but in practical applications, the RIP condition is proved to be an NP-hard problem, so an equivalent condition for non-coherence is proposed.

Definition 6: If the row vector $\{\phi_I\}$ in the observation matrix Φ cannot be represented by the column vector $\{\Psi_i\}$ in the sparse basis Ψ, and the column vector in the sparse basis Ψ cannot be represented by the row vector in the measurement matrix, the observation matrix Φ and the sparse basis Ψ means to be irrelevant. Non-coherent conditions can be measured by the degree of coherence, and the definition of correlation is as follows.

Definition 7: Φ is assumed as the observation matrix and Ψ as the sparse basis. The correlation between the observation matrix $\Phi = \{\phi_i\}_l^N$ and the sparse basis $\Psi = \{\psi_j\}_l^N$ is defined as:

$$\mu(\Phi, \Psi) = \sqrt{N} \cdot \max_{1 \leq i,j \leq N} \{|(\phi_i, \Psi_j)|\} \tag{5}$$

Correlation indicates the correlation between any row vector in the observation matrix ϕ and any column vector in the sparse basis Ψ. There is at least j making $|\langle \varphi_k, \Psi_j \rangle| \geq 1 \Big/ \sqrt{N}$, and then $\mu(\Phi, \Psi) \geq 1$, there is also any column vector in the observation matrix ϕ which satisfy the following condition.

$$\sum_{k=1}^{N} |\langle \varphi_k, \Psi_j \rangle|^2 = \|\Psi_j\|_{l_2}^2 = 1 \tag{6}$$

Therefore, $\mu(\Phi, \Psi) \leq \sqrt{N}$ and the range of the correlation is $1 \leq \mu(\Phi, \Psi) \leq \sqrt{N}$, when $\mu(\Phi, \Psi) = 1$, the maximum non-coherence between Φ and Ψ has been obtained. The less non-coherence between observation matrix and the sparse base, the compression ratio of the CS observation is larger, and the higher the probability for the reconstruction end which can achieve highly accurate reconstruction.

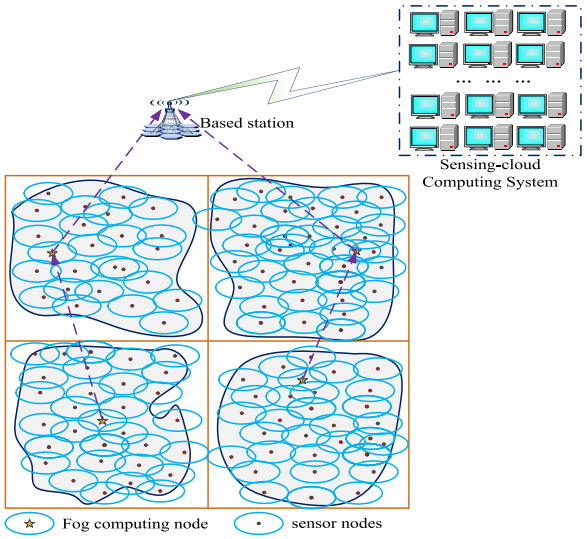

FIGURE 1. Schematic diagram of data migration mechanism-aware cloud computing.

Definition 8: Defining a random variable z as the ratio of the number of dropped packets in the sliding window to the window length, that is,

$$z = \frac{\sum_{i=1}^{L} (1 - X_i)}{L} \tag{7}$$

Figure 1 shows the principle diagram of the perceptual cloud computing of the data migration mechanism. The ''pentagram'' indicates a fog node, and the rest of them indicate sensor nodes. We divide the monitoring area into four equal coverage areas, and each area give a node clustering form and uploaded the collected data to the base station through the fog nodes. After the data fusion processing by the base station, the data is finally submitted to the perceptual cloud computing platform. In the following sections, we mainly study the routing mechanism of a certain coverage area.

B. METHODS AND ANALYSIS

We suppose that the sensor network randomly deploys N nodes, and its collected data is recorded as $d = (d_1, d_2, \ldots d_n)^T$, d is sparse under the sparse basis $\Psi_{N \times N}$, and the observation matrix is $\Phi = (\phi_{ij})_{M \times N}$, where $M \times N$ observation vector is $Y = (y_i)_{M \times 1} = \Phi \cdot \Psi^T \cdot d$, and then the Sink node can be reconstructed under certain accuracy constraints by solving the optimization problems shown in equations (8) and (9).

$$Y = \Phi \cdot S = \Phi \cdot \Psi^T \cdot d = \Theta \cdot d \tag{8}$$

$$\hat{d} = \arg\min \|d\|_l \quad s.t.\ Y = \Phi \cdot S \tag{9}$$

When the target node of interest enters the monitoring area at a certain speed, the defined target state are

$\boldsymbol{x}_t = [x_t, y_t, \dot{x}_t, \dot{y}_t]$ where $[x_t, y_t]$ and $[\dot{x}_t, \dot{y}_t]$ represent the target position and target speed at the k-th moment. The system state equation is shown in (10):

$$\boldsymbol{x_{k+1}} = \Psi_k \boldsymbol{x_k} + W_k \tag{10}$$

where, $\psi_{\boldsymbol{k}}$ is a state transfer matrix, W_k is process noise and Gaussian white noise, and its covariance matrix is Q.

$$\boldsymbol{F} = \begin{bmatrix} 1 & 0 & t & 0 \\ 0 & 1 & 0 & t \\ t & 0 & 1 & 0 \\ 0 & t & 0 & 1 \end{bmatrix} \tag{11}$$

$$Q = q \cdot \begin{bmatrix} \frac{t^3}{3} & 0 & \frac{t^2}{2} & 0 \\ 0 & \frac{t^3}{3} & 0 & \frac{t^2}{2} \\ \frac{t^2}{2} & 0 & \frac{t^3}{3} & 0 \\ 0 & \frac{t^2}{2} & 0 & \frac{t^3}{3} \end{bmatrix} \tag{12}$$

where t is the observation interval and q is the white noise parameter.

$$z_{k+1}^j = h_{k+1}^j + v_{k+1}^j = \arctan\left(\frac{x_{k+1} - x^j}{y_{k+1} - y^j}\right) + v_{k+1}^j \tag{13}$$

h_{k+1}^j is the ideal measurement, $[x^j, y^j]$ is the position of the j-th node, v_{k+1}^j is Gaussian noise, and its average value is 0, and the standard deviation is σ_v, i.e. $v_{k+1}^j \sim N\left(0, \sigma_v^2\right)$. Process noise and measurement noise are uncorrelated.

$x_{0:k}$ and $z_{1:k}$ represents the target state and measurement from 0 to k, and the initial joint probability density $p(x_0)$, noise model W_k and v_k are known. And then, the joint probability density of $(x_{0:k}, z1 : k)$ is known by Equation 14.

$$p\left(x_{0:k}, z_{1:k}\right) = p\left(x_0\right) \prod_{i=1}^{k} p\left(x_k \left| x_{k-1}\right.\right) \prod_{j=1}^{k} p\left(z_j, x_j\right) \tag{14}$$

The traditional Cramer-Rao lower bound on mean square error provides a performance limit for any unbiased estimation of fixed parameters. This article assumes $\hat{x}$ an estimate of x, and the posterior Cramer-Rao inequality gives the mean square error bound of the estimator as shown in Equation (15).

$$E\left\{\left[\hat{x}_k - x_k\right] \cdot \left[\hat{x}_k - x_k\right]^T\right\} \geq L^{-1}\left(x_k\right) \tag{15}$$

where L is the Fisher information matrix, $L = E\{\log p(x, z)\}$, where the expectation is about the joint probability density $p(x_{0:k}, z_{1:k})$.

In the traditional unconditional constraints, $x_{0:k}$ and $z_{1:k}$ are random vectors, and the boundary is obtained by averaging all $z_{1:k}$ and $x_{0:k}$. In fact, at time $k + 1$, it may be known in addition to the target state equation and measurement equation, and $z_{1:k}$. is also known.

Under all known past $z_{1:k}$ conditions, when a new measurement z_{k+1} arrives, the lower bound of the estimated target state satisfies the equation (16).

$$E\left\{\left[\hat{x}_k - x_k\right] \cdot \left[\hat{x}_k - x_k\right]^T \left| z_{1:k}\right.\right\} \geq L^{-1}\left(x_k \left| z_{1:k}\right.\right) \tag{16}$$

The measurement $z_{1:k}$ is a random vector, we use the target state estimate at time k to predict the performance lower bound of the target state estimate at time $k + 1$. Under known measurement $z_{1:k}$ conditions, the conditions of the mean square error of the target state vector x_{k+1} can be calculated as Equation (17):

$$L\left(x_{k+1} \left| z_{1:k}\right.\right) = M_k^{22} = M_k^{21}\left[L_A\left(x_k \left| z_{1:k}\right.\right) + M_k^{11}\right]^{-1} M_k^{12} \tag{17}$$

$$M_k^{11} = E_{p_{k+1}^c}\left[\log p\left(x_{k+1} \left| x_k\right.\right)\right] \tag{18}$$

$$M_k^{12} = E_{p_{K=1}^c}\left[-\log p\left(x_{k+1} \left| x_k\right.\right)\right] = \left(M_k^{21}\right)^T \tag{19}$$

$$M_k^{22} = E_{p_{k+1}^c}\left[\log p\left(x_{k+1} \left| x_k\right.\right)\right] + E_{p_{k+1}^c}\left[\log p\left(z_{k+1} \left| x_k\right.\right)\right] \tag{20}$$

where $p_{k+1}^c = p\left(x_{0:k+1}, z_{k+1} \left| z_{1:k}\right.\right)$. A more direct CPCRLB approximate iterative formula is provided in [17], as shown in equation (21):

$$L\left(x_{k+1} \left| z_{1:k}\right.\right) \approx M_k^{22} - M_k^{21}\left[L_A\left(x_k \left| z_{1:k-1}\right.\right) + M_k^{11}\right] M_k^{12} \tag{21}$$

According to the state model and measurement model of the target motion, this article can obtain L, as shown in equation (22):

$$L\left(x_{k+1} \left| z_{1:k}\right.\right) \approx \left[FL^{-1}\left(x_k \left| z_{1:k+1}\right.\right) F^T + Q\right]^{-1} + M_k^{22} \tag{22}$$

where $M_k^{22} = E_{p_{k+1}^c}\left[\log p\left(z_{k+1} \left| x_k\right.\right)\right]$, its initial iteration condition is $L\left(x_0 \left| z_{x-1}\right.\right) = E\left[\log p\left(x_0\right)\right]$.

The DOA-based target tracking system does not exist in a real mathematical expression of M_k^{22}. We assume that there are N_p particles with weights, it can be expressed $\{x_k^l, w_k^l\}_{t=1}^{N_p}$ at time k, the weight of these particles becomes $1/N_p$ after resampling, so at time k the posterior joint probability density function can be expressed as:

$$p\left(x_{0:k} \left| z_{1:k}\right.\right) \approx \frac{1}{N} \sum_{l=1}^{N_p} \delta\left(x_{0:k} - x_{0:k}^l\right) \tag{23}$$

At the same time, according to the measurement model, the likelihood function can be obtained as follows.

$$\ln p\left(z_{k+1} \left| x_{k+1}\right.\right) = \sum_{j=1}^{N_p}\left[-\frac{\left(z_{k+1}^j - j_{k+1}^j\right)}{2\sigma_v^2} - \ln\sqrt{2\pi}\sigma_v\right] \tag{24}$$

And the elements of matrix M_k^{22} can be expressed as follows.

$$M_k^{22} = \begin{bmatrix} M_k^{22}(1,1) & M_k^{22}(1,2) & 0 & 0 \\ M_k^{22}(2,1) & M_k^{22}(2,2) & 0 & 0 \\ 0 & 0 & M_k^{22}(3,3) & M_k^{22}(3,4) \\ 0 & 0 & M_k^{22}(4,3) & M_k^{22}(4,4) \end{bmatrix} \tag{25}$$

where,

$$M_k^{22}(1,1) = \frac{1}{N_p\sigma_v^2}\sum_{i=1}^{N_p}\sum_{j=1}^{N_a}\frac{(y_{k+1}-y^i)^2}{\left[(x_{k+1}-x^i)^2+(y_{k+1}-y^i)^2\right]^2}\Bigg|_{x_{k+1}=x_{k+1}^i} \tag{26}$$

$$M_k^{22}(1,2) = \frac{1}{N_p\sigma_v^2}\sum_{i=1}^{N_p}\sum_{j=2}^{N_a}\frac{(y_{k+1}-y^i)(x_{k+1}-x^i)}{\left[(x_{k+1}-x^i)^2+(y_{k+1}-y^i)^2\right]^2}\Bigg|_{x_{k+1}=x_{k+1}^i} \tag{27}$$

$$M_k^{22}(2,1) = \frac{1}{N_p\sigma_v^2}\sum_{i=2}^{N_p}\sum_{j=1}^{N_a}\frac{(x_{k+1}-x^i)^2}{\left[(x_{k+1}-x^i)^2+(y_{k+1}-y^i)^2\right]^2}\Bigg|_{x_{k+1}=x_{k+1}^i} \tag{28}$$

$$M_k^{22}(2,2) = \frac{1}{N_p\sigma_v^2}\sum_{i=2}^{N_p}\sum_{j=2}^{N_a}\frac{(x_{k+1}-x^i)(y_{k+1}-y^i)}{\left[(x_{k+1}-x^i)^2+(y_{k+1}-y^i)^2\right]^2}\Bigg|_{x_{k+1}=x_{k+1}^i} \tag{29}$$

IV. IMPLEMENTATION OF IM-CSR ALGORITHM

A. LEVEL DETERMINATION OF THE LOCAL DENSITY FOR MONITORING TARGET

The load balancing mechanism deploys sensor nodes based on the distribution of monitoring targets. This deployment solution not only completes the basic tasks of node deployment, i.e. coverage and connectivity, but also achieves load balancing at various locations. In short, we investigate the density of monitoring targets at various locations, deploy more nodes in dense locations, and deploy fewer nodes in sparse locations.

We determine a uniform local range σ of the entire network, and calculate the number of monitoring targets in the local range σ at any position x in the entire network as the local density ρ_x of the monitoring targets at that position. If the local density exceeds the threshold ϕ, and then the actual required sensing radius r_x. of the sensor node is reduced.

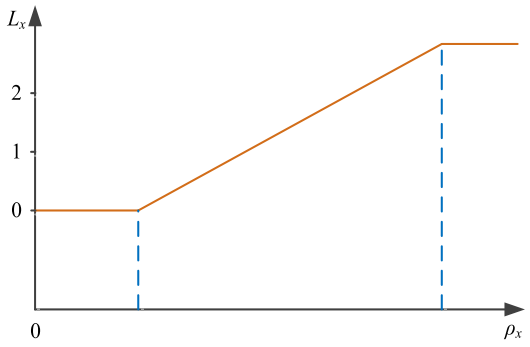

FIGURE 2. Comparison of L_x and ρ_x.

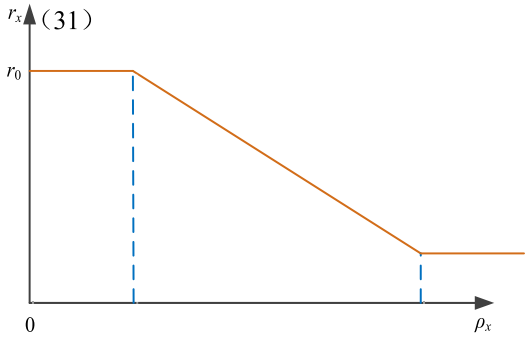

FIGURE 3. Comparison of r_0 and ρ_x.

We set the local density level L_x of the monitoring target as in equation (30), as show in Fig2.

$$L_x = \begin{cases} 0, & \text{if } \rho_x < \Phi 1 \\ \dfrac{\rho_x - \Phi 1}{\Delta\rho}, & \text{if } \Phi 1 \le \rho_x \le \Phi 2 \\ L_{\max} & \text{if } \rho_x > \Phi 2 \end{cases} \tag{30}$$

The actual required sensing radius of the sensor node at position x is shown in equation (31).

$$r_x = \begin{cases} r_0 & \text{if } r_0 < \rho_x \\ r_0 - L_x \times \Delta r & \text{if } r_0 = \rho_x \\ r_{\max} & \text{if } r_0 > \rho_x \end{cases} \tag{31}$$

where Δr represents a basic unit with a reduced sensing radius. The following figure showsthe relationship between the actual required sensing radius and local density. Because the monitoring targets are distributed on the grid, there is an upper limit on the local density of the monitoring targets and an upper limit on the local density level. The actual required sensing radius also has an upper limit, i.e., it must meet $r_x > 0$, as show in Fig3.

Monitoring targets may be located in different isolated areas. An isolated area is randomly selected, and the location, where the local density of the monitoring target is relatively large, is deployed to deploy the first sensor node. The greedy method based on the local density of the monitoring target is used for tackling the coverage problem of other locations in this area [48], [49]. Specifically, within the maximum

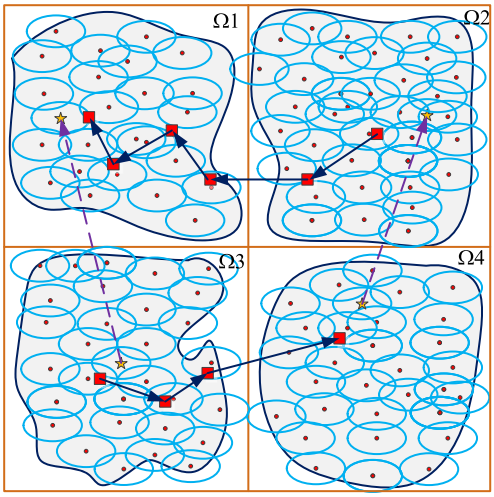

FIGURE 4. Processing of target migration coverage.

communication range $R_{\max}$ of the currently deployed sensor node locations x_i, the location x_{i+1} with the highest local density of the monitoring target is selected as the deployment location of the next sensor node, that is,

$$x_{i+1} = \arg\{N(x_{i+1})\} \tag{32}$$

$$d(x_i, x_{i+1}) \leq R_{\max} \tag{33}$$

If the local density of monitoring targets of all locations within the maximum communication range around the current sensor node is zero, the previously deployed sensor node location is felled back and is used as the current position, and then the new position will be selected to deploy the sensor node. If the local density of monitoring targets within the maximum communication range of all previously deployed sensor node locations is zero, a sensor node is deployed in any of the isolated areas that can cover the monitoring target by a hopping way and sensor nodes continue to be deployed by new position until all monitoring targets throughout the network are covered.

It is worth noting that each time a sensor node is deployed at any location to complete the coverage task, the actual required sensing range of that location is used as its sensing range to achieve load balancing, as shown in Figure 4. In addition, each time a sensor node is deployed, the number of deployed sensor nodes and the number of remaining monitoring targets must be updated.

More specifically, for any two segments S_u and S_v, we need to find the specific grid cells Ω_i and Ω_j that can satisfy

$$\begin{cases} \Omega_i = \arg\{\min d(S_u, S_v)\} \\ \Omega_j = \arg\{\min d(S_u, S_v)\} \end{cases} \tag{34}$$

where

$$\begin{aligned} &d(S_u, S_v) = d(\Omega_i, \Omega_j) \\ &\text{subject to } \Omega_i \in S_u \\ &\qquad\qquad \Omega_j \in S_v \end{aligned} \tag{35}$$

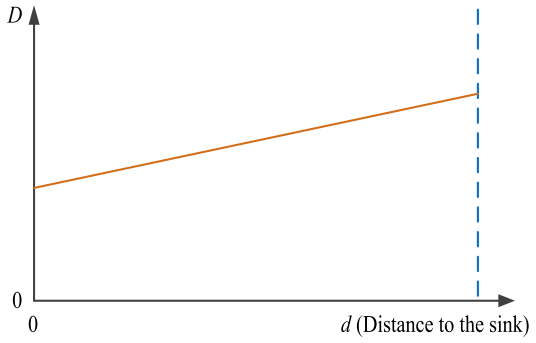

FIGURE 5. The reference transmission distance.

where $d(\Omega_i, \Omega_j)$ is the distance between the centers of the two grid cells Ω_i and Ω_j.

B. TRANSMISSION DISTANCE CONTROL MECHANISM

In order to improve network life, two factors must be met, the first factor is to minimize energy consumption, and the other one is to balance energy consumption. Therefore we have designed two transmission distances in transmission. One is the minimum distance for energy consumption, and the other is the energy balance distance. Both distances guide the data transmission route.

(1) Reference Transmission Distance

The reference transmission distance is used to fit a linearly increasing distance set for load balancing, as show in Fig5.

$$D = d_0 + ad \tag{36}$$

where d is the distance to the sink. It can be seen from the Figure 5, the farther away from the base station sink, the larger the reference transmission distance. After the nodes are deployed, clustering is performed, and data is transmitted by clusters. The way in which each cluster chooses a route is considered based on two factors, the reference transmission distance and the amount of data received. Specifically, the cluster head X_i selects the next hop cluster head X_j according to the following formula.

$$f(j) = c_1 \frac{\varphi(j)}{\varphi_{\max}} + c_2 \frac{|D_i - d(i,j)|}{d_{\max}} \tag{37}$$

where $\varphi(j)$ represents the amount of data received by the cluster head, and $d(i, j)$ represents the distance between clusters i and j. The first denominator represents the product of the number of monitoring targets and the data generation rate, i.e., the total amount of data, and the second denominator represents the maximum distance between the node and the base station sink.

In the above formulas, j with the smallest function value is selected as the relaying node of i. Obviously, if the relaying node forwards a smaller amount of data, the closer the distance between the cluster heads X_i and X_j is near to the reference distance, and then the more likely the node X_j is selected as the relaying node.

In order to further realize load balancing across the network, we propose a data traffic transferring mechanism. The core idea of this mechanism is to deploy sensor nodes among different groups with large traffic differences to create an additional path to transfer part of the data from the group with higher traffic to the group with smaller traffic, thereby balancing the load of different regions. This data traffic transferring mechanism involves both node deployment and data transmission.

(1) Representation for data flow level

To reduce the computational complexity, the communication load is calculated by each group Ω_i as the unit. The data traffic level of a group is as followed.

$$\xi(\Omega_i) = \frac{\sum_{j \in LH(G_i)} \varphi(j)}{B(\Omega_i)} \tag{38}$$

where $\phi(j)$ represents the amount of data forwarded by the cluster of the last hop (which is directly sent to the base station), $LH(\Omega_i)$ represents the set of cluster j of the last hop in group Ω_i, and $B(\Omega_i)$ represents the number of cluster j of the last hop in group Ω_i. The above formula represents the average data forwarding volume of cluster j in the last hop of group Ω_i.

(2) Determine of the location for traffic transfer

This is how the start and end positions of the data transfer route are chosen. We use the following function to judge.

Prerequisites for traffic transfer (from cluster Ω_i to cluster Ω_j):

$$\begin{cases} \xi(\Omega_u) - \xi(\Omega_v) > \xi_0 \\ \varphi(i) - \varphi(j) > \varphi_0, \quad i \in \xi(\Omega_u),\ j \in \xi(\Omega_v) \\ d(i,j) < d_0, \quad i \in \xi(\Omega_u),\ j \in \xi(\Omega_v) \\ d(i, \text{sink}) > L_0, \quad d(j, \text{sink}) > L_0 \end{cases} \tag{39}$$

Determination of the start position (cluster Ω_i) and end position (cluster Ω_j) of the traffic transfer.

$$\left(\Omega_i, \Omega_j\right) = \max g(\Omega_i, \Omega_j) \tag{40}$$

$$g(\Omega_i, \Omega_j) = \frac{\varphi(\Omega_i) - \varphi(\Omega_j)}{d(\Omega_i, \Omega_j)} \tag{41}$$

The numerator is the difference in data forwarding traffic between the two clusters, and the denominator is the distance between the two clusters. Obviously, the larger the difference, the smaller the distance, i.e., the smaller the cost, and then the more suitable for data traffic transfer.

V. PERFORMANCE EVALUATION

We compare CSR-IM with the following algorithms: DMOA [30], TBSR [31], and MDCS [32]. DMOA is a non-clustering algorithm for event-driven sensor networks, and TBSR is a dynamic clustering algorithm based on events, both of which use fixed base stations. MDCS are non-clustered algorithms using mobile base stations, while CSR-IM is a combination of cluster and mobile base station technology. Through the experimental comparison among them, the advantages brought by clustering and base station movement can be clearly demonstrated.

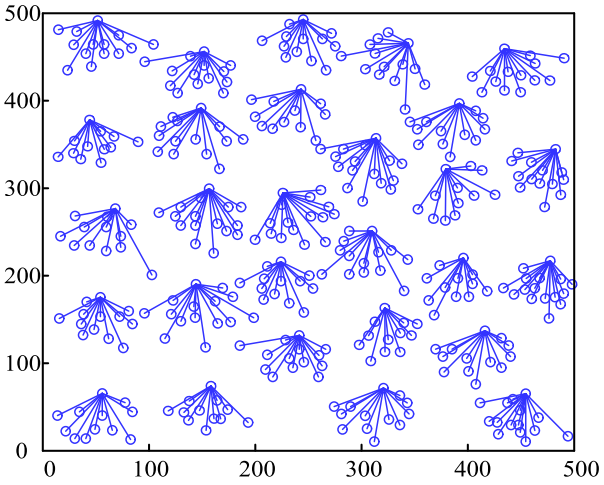

FIGURE 6. CSR-IM clustering results at t = 100s.

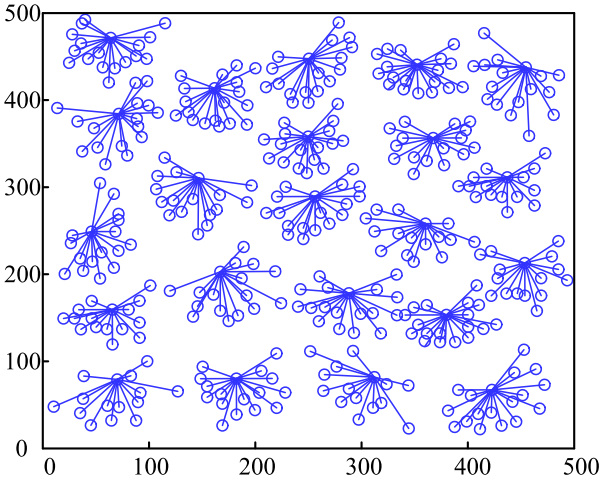

FIGURE 7. CSR-IM clustering results at t = 300s.

With the purpose of convenient comparison, we use the wireless network energy consumption model in [19]. And we assume that the shape of the event domain is square, and the location, time, and duration of the event are random. CSR-IM and DMOA aggregate data in the cluster and the experiment considers different data aggregation rates.

The clustering results of the CSR-IM algorithm at different times are shown in Figure 6 to Figure 8. In the simulation, the sensor nodes are randomly deployed in the square monitoring area. The CSR-IM algorithm fully considers the distance relationship between the cluster head and other nodes. At the same time, more attention is paid to the remaining energy of the node and the position of the base station, and the selected cluster head is more biased towards the base station, so the energy consumption of the members in the cluster to transmit data to the cluster head will be reduced.

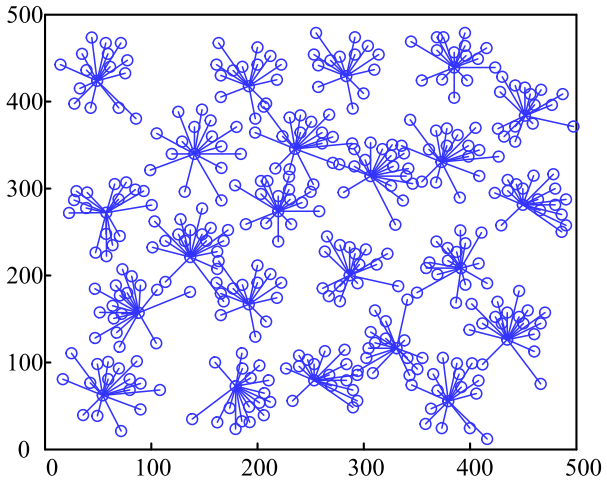

FIGURE 8. Figure 6 CSR-IM clustering results at t = 500s.

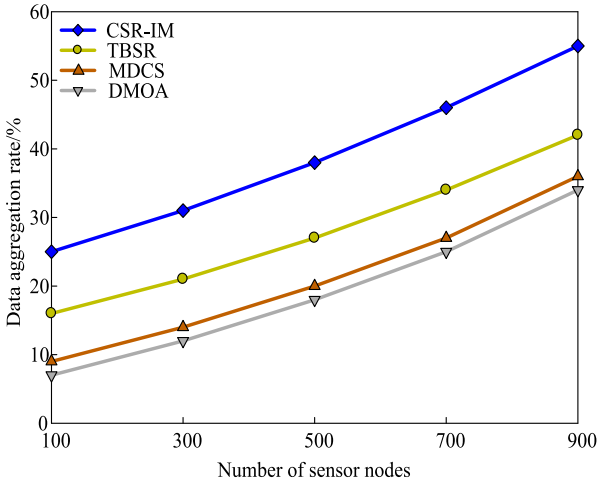

FIGURE 10. Comparison of data aggregation rate of four algorithms (t = 300s).

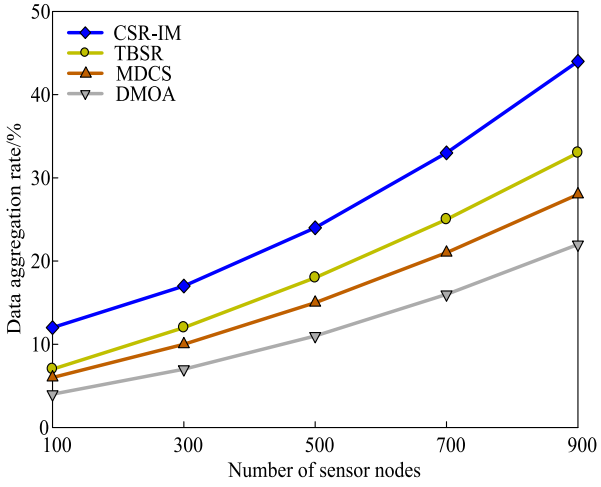

FIGURE 9. Comparison of data aggregation rate of four algorithms (t = 100s).

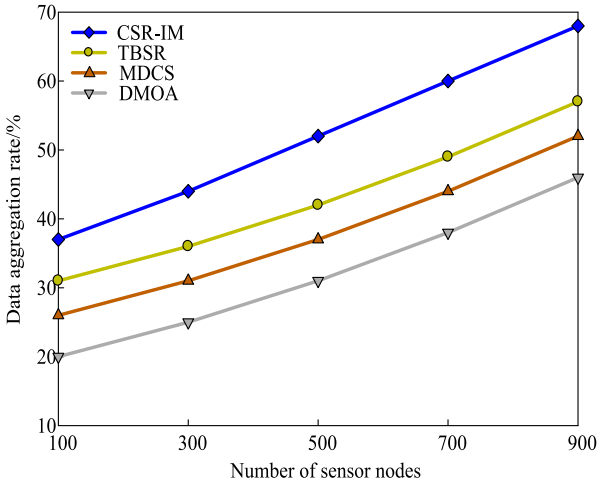

FIGURE 11. Comparison of data aggregation rate of four algorithms (t = 500s).

The CSR-IM algorithm has randomness in the number of clusters, the number of nodes in the cluster is uneven, and the cluster and cluster coverage is relatively even, which balances the data transmission energy consumption of the nodes in the cluster. The DMOA algorithm given in [30] uses the dual cluster head method. The primary and secondary cluster heads have a clear division of labor. Due to different clustering reasons for reference, the main cluster head selection of the DMOA algorithm is based on the distance from the cluster center The remaining energy is used as a reference standard, so it is closer to the center of the cluster, and the secondary cluster head uses the remaining energy and the distance to the base station point as reference factors in the election, so the selected secondary cluster head is closer to the base station.

When $E = 5$J, the data aggregation rate of each algorithm is shown in Figure 9-13 under the number of sensor nodes at different times. It can be seen from the simulation results that the CSR-IM algorithm has a higher data aggregation rate than the other three algorithms at different times. At the initial moment of the network, due to the difference between network connectivity and the state of the sensor nodes, the aggregation rate of all algorithms is poor. As the number of sensor nodes increases, the advantages brought by data aggregation gradually increase, compared to CSR-In terms of IM algorithm and TBSR algorithm, the performance enhancement speed of MDCS and DMOA is relatively slow, and the difference in data aggregation rate between the two algorithms is small. The main reasons are as follows. First, the cluster-based event information reporting mechanism of CSR-IM reduces the number of control messages related to event information acquisition, and the data aggregation within the cluster reduces the transmission of redundant data. Second, the data migration mechanism can make more nodes have the opportunity to become one-hop neighbors of

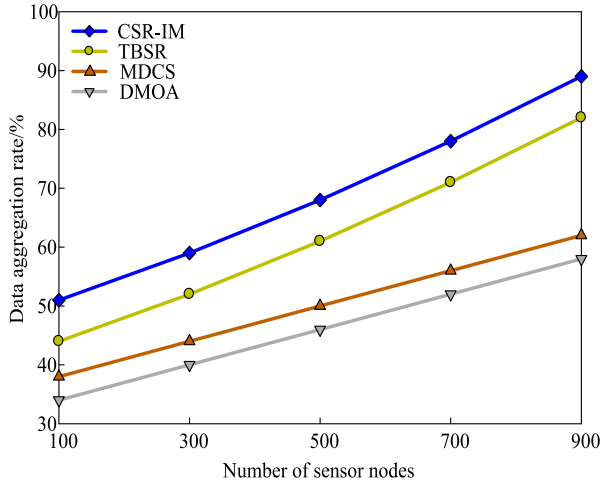

FIGURE 12. Comparison of data aggregation rate of four algorithms (t = 700s).

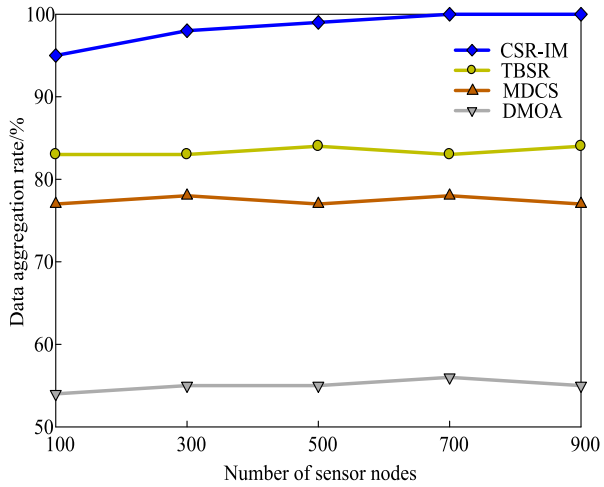

FIGURE 13. Comparison of data aggregation rate of four algorithms (t = 900s).

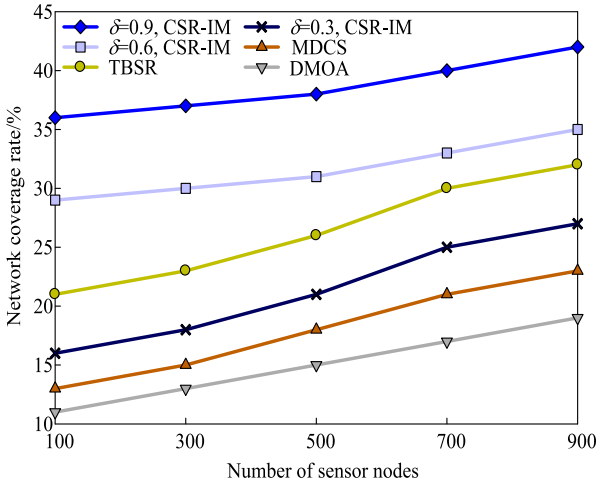

FIGURE 14. Comparison of network coverage of four algorithms (t = 100s).

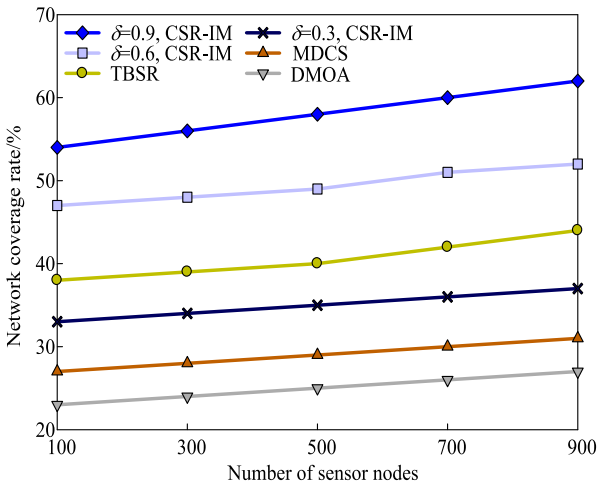

FIGURE 15. Comparison of network coverage of four algorithms (t = 300s) .

the base station. Third, the data information obtained based on the number, location, and average energy of the event domain nodes enables the fog nodes to accurately grasp the optimal location. That is to shorten the data transmission distance and better balance energy consumption. The comparison results between different numbers of sensor nodes and data aggregation rate under different time effects show that the data aggregation rate of the CSR-IM algorithm proposed in this paper is higher than the other three algorithms. At different times, they were higher than 7.89%, 8.05%, 8.13%, 8.39%, and 8.51%, respectively, and their data aggregation rates increased by 8.19% on average.

In order to investigate the effect of sensor nodes on network coverage, we used different parameter values as the basis for calculation in the experiments. We calculated the network coverage of four algorithms when the parameters changed. The results are shown in Figure 14 to Figure 18. With the increase of the number of sensor nodes, the network coverage of four algorithms has increased, but with the passage of time, the improvement of the MDCS algorithm and the DMOA algorithm has gradually flattened. The main reasons are as follows. First, the CSR-IM algorithm in this paper uses a dynamic migration mechanism. In the unit cycle, the fog node recalculates the speed and position of the target node to make it more accurately calculate the trajectory of the target node. Second, as the dynamic parameters increase, the corresponding time among sensor nodes is shortened, and the network coverage changes significantly. Third, when the target node is located in the event domain, the clustering structure and the state transition among sensor nodes can effectively reduce the amount of data transmission in the network, thereby extending the network lifetime. Fourth, the CSR-IM algorithm in this article has used the data aggregation mechanism. When the data aggregation rate is small, the abnormal death of nodes

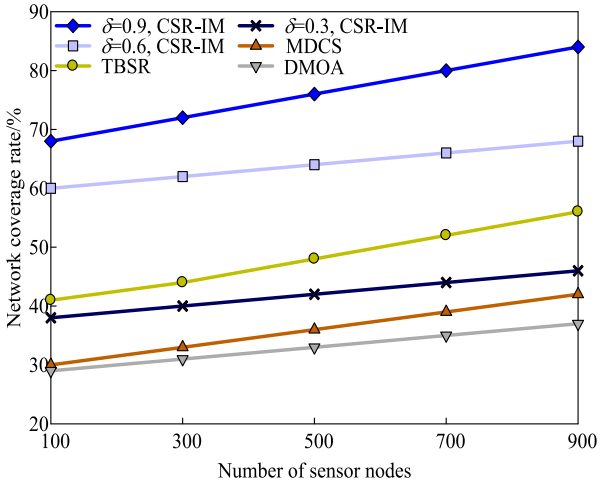

FIGURE 16. Comparison of network coverage of four algorithms (t = 500s).

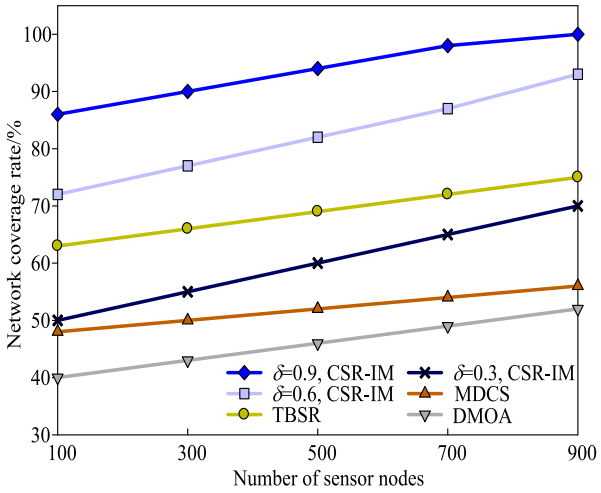

FIGURE 17. Comparison of network coverage of four algorithms (t = 700s).

in the event domain has a small impact on the reduction of the amount of data in the network. At the same time, the migration strategy of the CSR-IM algorithm suppresses the probability of abnormal death nodes. Therefore, the CSR-IM algorithm's network coverage will increase as the parameter value increases. The other three algorithms increase network coverage by increasing the number of sensor nodes, and do not consider the impact of data redundancy on network coverage, which results to a slow increase in the network coverage of the three algorithms. The CSR-IM algorithm has three different coverage effects at the same time when we set δ to 0.3, 0.6 and 0.9. When the number of sensor nodes is 500 to 700, the network coverage of the CSR-IM algorithm has a great advantage. The other three algorithms cannot obtain higher network coverage by changing the dynamic parameters. Based on the analysis of Figure 14 to Figure 18, the network coverage has increased by 12.02%, 12.56%, 12.77%, 12.86%, and 13.05%,

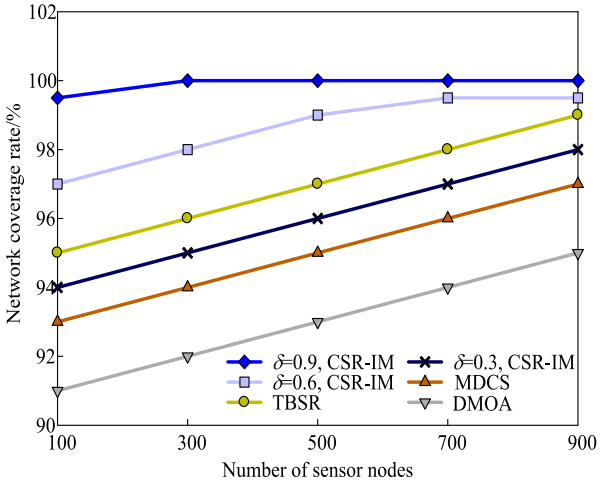

FIGURE 18. Comparison of network coverage of four algorithms (t = 900s).

respectively, and its network coverage has increased by 12.65% on average.

VI. CONCLUSION

This paper studies dynamic data aggregation routing and network coverage with migration mechanism, and proposes the Compressed Sensing Routing-control- method with Intelligent Migration-mechanism based on Sensing Cloud-computing. First, when the dynamic target node reaches a new location, the CSR-IM algorithm establishes a full-network routing tree with the fog node as the root, and at the same time, clusters the nodes in the event domain with distributed way. When an event occurs or ends, the accurate and optimal position of the event information is calculated according to the compressed sensing theory, which effectively shortens the data transmission distance and balances the network load, extending the network life cycle. Second, the CSR-IM algorithm uses dynamic parameter thresholds to improve network coverage, and at the same time which can effectively calculate the new location information of the moving target node and reduce unnecessary location calculations, thereby reducing the computational complexity. Third, the CSR-IM algorithm provides a data migration mechanism, which can quickly determine the location information of the target node through the perception among sensor nodes, and avoid data loss during the movement process. For the transmission of data within the network, the CSR-IM algorithm aggregates data within the cluster and can reliably transmit the aggregated data. And when a node dies, the CSR-IM algorithm can simply and effectively complete route repair. Finally, algorithm analysis and simulation experiments show that the CSR-IM algorithm can effectively reduce the average energy consumption of data packets, improve the data aggregation rate and coverage rate, and then extend the network life cycle. It has laid a certain foundation for the research of heterogeneous sensor networks. How to use multiple base

stations to comprehensively improve the performance of ultra-large- scale WSNs is the next research focus.

REFERENCES

[1] T. Wang, Y. Mei, W. Jia, X. Zheng, G. Wang, and M. Xie, "Edge-based differential privacy computing for sensor–cloud systems," *J. Parallel Distrib. Comput.*, vol. 136, pp. 75–85, Feb. 2020.
[2] C. Yewang, Z. Lida, P. Songwen, Y. Zhiwei, C. Yi, L. Xin, D. Jixiang, and X. Naixue, "KNN-BLOCK DBSCAN: Fast clustering for large scale data," *IEEE Trans. Syst., Man, Cybern., Syst.*, to be published, doi: 10.1109/TSMC.2019.2956527.
[3] X. Liu, T. Qiu, and T. Wang, "Load-balanced data dissemination for wireless sensor networks: A nature-inspired approach," *IEEE Internet Things J.*, vol. 6, no. 6, pp. 9256–9265, Dec. 2019.
[4] W. Tian, B. M. Z. Alam, W. Guojun, Q. Lianyong, W. Jie, and H. Thaier, "Preserving balance between privacy and data integrity in edge-assisted Internet of Things," *IEEE Internet Things J.*, to be published, doi: 10.1109/JIOT.2019.2951687.
[5] Z. Sun, Y. Zhang, Y. Nie, W. Wei, J. Lloret, and H. Song, "CASMOC: A novel complex alliance strategy with multi-objective optimization of coverage in wireless sensor networks," *Wireless Netw.*, vol. 23, no. 4, pp. 1201–1222, May 2017.
[6] P. Songwei, S. Tianma, W. Xiaorong, G. Chunhua, N. Zhong, Y. Xiaochun, and X. Naixue, "3DACN: 3D augmented convolutional network for time series data," *Inf. Sci.*, to be published, doi: 10.1016/j.ins.2019.11.040.
[7] G. Zhao, H. Guo, Z. Sun, and W. Zheng, "A novel threshold-controllable algorithm for moving target coverage," *J. Eng. Sci. Technol. Rev.*, vol. 11, no. 2, pp. 1–7, 2018.
[8] Q. Mao, F. Hu, and Q. Hao, "Deep learning for intelligent wireless networks: A comprehensive survey," *IEEE Commun. Surveys Tuts.*, vol. 20, no. 4, pp. 2595–2621, 4th Quart., 2018.
[9] W. Tian, Q. Lei, S. A. Kumar, L. Anfeng, B. M. Z. Alam, and M. Ying, "Edge computing based trustworthy data collection model in the Internet of Things," *IEEE Internet Things J.*, to be published, doi: 10.1109/JIOT.2020.2966870.
[10] T. Wang, L. Qiu, G. Xu, A. K. Sangaiah, and A. Liu, "Energy-efficient and trustworthy data collection protocol based on mobile fog computing in Internet of Things," *IEEE Trans. Ind. Informat.*, to be published, doi: 10.1109/tii.2019.2920277.
[11] Y. Chen, X. Hu, W. Fan, L. Shen, Z. Zhang, X. Liu, J. Du, H. Li, Y. Chen, and H. Li, "Fast density peak clustering for large scale data based on kNN," *Knowl.-Based Syst.*, vol. 187, Jan. 2020, Art. no. 104824, doi: 10.1016/j.knosys.2019.06.032.
[12] L. Xiaoyang, Z. Yanming, K. Linghe, L. Cong, G. Yu, A. V. Vasilakos, and W. Minyou, "CDC: Compressive data collection for WSNss," *IEEE Trans. Parallel Distrib. Syst.*, vol. 26, no. 8, pp. 2188–2197, Aug. 2015.
[13] Liu Chang, Yao Xiangju, and Luojuan, "Multiregional secure localization using compressive sensing in wireless sensor networks," *ETRI J.*, vol. 41, no. 6, pp. 739–749, Dec. 2019.
[14] R. Banerjee and S. Das Bit, "Low-overhead video compression combining partial discrete cosine transform and compressed sensing in WMSNs," *Wireless Netw.*, vol. 25, no. 8, pp. 5113–5135, Nov. 2019.
[15] Sun, Li, Wei, Li, Min, and Zhao, "Intelligent sensor-cloud in fog computer: A novel hierarchical data job scheduling strategy," *Sensors*, vol. 19, no. 23, p. 5083, Nov. 2019.
[16] U. S. Pacharaney and G. R. Kumar, "Clustering and compress data gathering in WSNss," *Wireless Pers. Commun.*, vol. 109, no. 2, pp. 1311–1331, Nov. 2019.
[17] X. Gu, X. Zhou, B. Yuan, and Y. Sun, "A Bayesian compressive data gathering scheme in wireless sensor networks with one mobile sink," *IEEE Access*, vol. 6, pp. 47897–47910, 2018.
[18] H. Jingfei, Z. Yatong, S. Guiling, and X. Yi, "Compressive multi-attribute data gathering using Hankel matrix in wireless sensor networks," *IEEE Commun. Lett.*, vol. 23, no. 12, pp. 2417–2421, Dec. 2019.
[19] S. Zeyu, L. Longxing, X. Xiaofei, L. Zhiguo, and N. N. Xiong, "A novel nodes deployment assignment scheme with data association attributed in WSNss," *J. Internet Technol.*, vol. 20, no. 2, pp. 509–520, 2019.
[20] L. Xuewen, X. Song, and Q. Lei, "Optical SDMA for applying compressive sensing in WSN," *J. Syst. Eng. Electron.*, vol. 27, no. 4, pp. 780–789, Aug. 2016.
[21] X. Liu, "A deployment strategy for multiple types of requirements in wireless sensor networks," *IEEE Trans. Cybern.*, vol. 45, no. 10, pp. 2364–2376, Oct. 2015.
[22] S. Zeyu, Y. Yali, S. Houbing, and W. Huihui, "CCAJS: A novel connect coverage algorithm based on joint sensing model for wireless sensor networks," *KSII Trans. Internet Inf. Syst.*, vol. 10, no. 10, pp. 5014–5034, Oct. 2016.
[23] H. Zhe, Z. Xia, Z. Dalong, Z. Ce, and D. Siyuan, "A data gathering algorithm based on compressive sensing in lossy wireless sensor networks," in *Proc. 2nd Int. Conf. Frontiers Sensors Technol. (ICFST)*, Shenzhen, China, Apr. 2017, pp. 146–153.
[24] Y. Wu, H. Huang, Q. Wu, A. Liu, and T. Wang, "A risk defense method based on microscopic state prediction with partial information observations in social networks," *J. Parallel Distrib. Comput.*, vol. 131, pp. 189–199, Sep. 2019.
[25] T. Wang, H. Luo, W. Jia, A. Liu, and M. Xie, "MTES: An intelligent trust evaluation scheme in sensor-cloud enabled industrial Internet of Things," *IEEE Trans. Ind. Informat.*, vol. 16, no. 3, pp. 2054–2062, Mar. 2020.
[26] Z. Sun, X. Xing, B. Song, Y. Nie, and H. Shao, "Mobile intelligent computing in Internet of Things: An optimized data gathering method based on compressive sensing," *IEEE Access*, vol. 7, pp. 66110–66122, 2019.
[27] L. Xuxun, W. Tian, J. Weijia, and L. Anfeng, "Quick convex hull-based rendezvous planning for delay-harsh mobile data gathering in disjoint sensor networks," *IEEE Trans. Syst., Man, Cybern., Syst.*, to be published, doi: 10.1109/TSMC.2019.2938790.
[28] W. Tian, L. Hao, Z. J. Xi, and X. Mande, "Crowdsourcing mechanism for trust evaluation in CPCS based on intelligent mobile edge computing," *ACM Trans. Intell. Syst. Technol.*, vol. 10, no. 6, pp. 1–19, Nov. 2019.
[29] S. Zeyu, Z. Guozeng, and X. Xiaofei, "ENCP: A new energy-efficient nonlinear coverage control protocol in mobile sensor networks," *EURASIP J. Wireless Commun. Netw.*, vol. 2018, pp. 1–15, Dec. 2018.
[30] N. Yalin, W. Haijun, Q. Yujie, and S. Zeyu, "Distributed and morphological operation-based data collection algorithm," *Int. J. Distrib. Sensor Netw.*, vol. 13, no. 7, pp. 1–16, Jul. 2017.
[31] T. Jiawei, L. Anfeng, Z. Jian, N. N. Xiong, Z. Zhiwen, and W. Tian, "A trust-based secure routing scheme using the traceback approach for energy-harvesting wireless sensor networks," *Sensors*, vol. 18, no. 3, pp. 1–43, Mar. 2018.
[32] W. Tian, Z. Dan, C. Shaobin, J. Weijia, and L. Anfeng, "Bidirectional prediction based underwater data collection protocol for end-edge-cloud orchestrated system," *IEEE Trans. Ind. Informat.*, to be published, doi: 10.1109/TII.2019.2940745.
[33] N. Yalin, L. Sanyang, C. Zhibin, and Q. Xiaogang, "Data preprocessing algorithm for better Haar-based data compression in wireless sensor networks," *Sensor Lett.*, vol. 12, no. 2, pp. 287–293, Feb. 2014.
[34] S. Zeyu, X. Xiaofei, W. Tian, L. Zhiguo, and Y. Ben, "An optimized clustering communication protocol based on intelligent computing information-centric Internet of Things," *IEEE Access*, vol. 7, pp. 28238–28249, 2019.
[35] X. Liu, T. Qiu, X. Zhou, T. Wang, L. Yang, and V. Chang, "Latency-aware path planning for disconnected sensor networks with mobile sinks," *IEEE Trans. Ind. Informat.*, vol. 16, no. 1, pp. 350–361, Jan. 2020, doi: 10.1109/tii.2019.2916300.
[36] S. Zeyu, T. Rong, X. Naixue, and P. Xiaoyan, "CS-PLM: Compressive sensing data gathering algorithm based on packet loss matching in sensor networks," *Wireless Commun. Mobile Comput.*, vol. 2018, Aug. 2018, Art. no. 5131949.
[37] L. Tang, W. Baijun, W. Hongyi, and P. Jian, "Low-cost collaborative mobile charging for large-scale WSNss," *IEEE Trans. Mobile Comput.*, vol. 16, no. 8, pp. 2213–2227, Aug. 2017.
[38] N. Yalin, W. Haijun, and Q. Yujie, "Data-smoothness based preprocessing strategy for wavelet data processing in WSNss," *J. Commun.*, vol. 9, no. 10, pp. 762–770, Oct. 2014.
[39] Y. Wu, H. Huang, N. Wu, Y. Wang, M. Z. A. Bhuiyan, and T. Wang, "An incentive-based protection and recovery strategy for secure big data in social networks," *Inf. Sci.*, vol. 508, pp. 79–91, Jan. 2020.
[40] W. Tian, K. Haoxiong, Z. Xi, W. Kun, S. A. Kumar, and L. Anfeng, "Big data cleaning based on mobile edge computing in industrial sensor-cloud," *IEEE Trans. Ind. Informat.*, vol. 16, no. 2, pp. 1321–1329, Sep. 2020.
[41] S. Zeyu, Z. Guozeng, and P. Xiaoyan, "PM-LPDR: A prediction model for lost packets based on data reconstruction on lossy links in sensor networks," *Int. J. Comput. Sci. Eng.*, vol. 19, no. 2, pp. 177–188, 2019.
[42] L. Xuxun, L. Anfeng, Q. Tie, D. Bin, W. Tian, and Y. Lei, "Restoring connectivity of damaged sensor networks for long-term survival in hostile environments," *IEEE Internet Things J.*, to be published, doi: 10.1109/JIOT.2019.2953476.

[43] Y. Xiaohan and B. S. Jun, "Joint routing and scheduling for data collection with compressive sensing to achieve order-optimal latency," *Int. J. Distrib. Sensor Netw.*, vol. 13, no. 10, pp. 1–13, Oct. 2017.
[44] J. Yun, Y. Jiangyu, and X. Huan, "Performance optimization based on compressive sensing for wireless sensor networks," *Wireless Pers. Commun.*, vol. 95, no. 3, pp. 1927–1941, Aug. 2017.
[45] L. Chengtie, W. Jinkuan, and L. Mingwei, "An efficient cross-layer optimization algorithm for data transmission in wireless sensor networks," *Int. J. Wireless Inf. Netw.*, vol. 24, no. 4, pp. 462–469, Dec. 2017.
[46] S. V. Kumar, V. Shekhar, and K. Manish, "ODECS: An on-demand explosion-based compressed sensing using random walks in wireless sensor networks," *IEEE Syst. J.*, vol. 13, no. 3, pp. 2466–2475, Sep. 2019.
[47] J. Li, C. Wang, Q. Zheng, and Z. Qian, "Leakage localization for long distance pipeline based on compressive sensing," *IEEE Sensors J.*, vol. 19, no. 16, pp. 6795–6801, Aug. 2019.
[48] X. Wang, Q. Zhou, Y. Gu, and J. Tong, "Compressive sensing-based data aggregation approaches for dynamic WSNs," *IEEE Commun. Lett.*, vol. 23, no. 6, pp. 1073–1076, Jun. 2019.
[49] Z. Sun, H. Wang, B. Liu, C. Li, X. Pan, and Y. Nie, "CS-FCDA: A compressed sensing-based on fault-tolerant data aggregation in sensor networks," *Sensors*, vol. 18, no. 11, p. 3749, Nov. 2018.

ZEYU SUN received the B.S. degree in computer science and technology from the Henan University of Science and Technology, in 2003, the M.Sc. degree from Lanzhou University, in 2010, and the Ph.D. degree from Xi'an Jiaotong University, in 2017. He is currently an Associate Professor with the School of Computer and Information Engineering, Luoyang Institute of Science and Technology, Luoyang, Henan, China. At the same time, he is also an External Tutor of master's students with the School of Information Engineering, Henan Institute of Science and Technology, Xinxiang, Henan. His research interests include wireless sensor networks, mobile computing, and the Internet of Things.

JUN LIU received the B.S. degree in computer science and technology from the Zhengzhou University of Light Industry, in 2000, and the M.Sc. degree from the Huazhong University of Science and Technology, in 2009. She is currently a Lecturer with the School of Computer and Information Engineering, Luoyang Institute of Science and Technology, Luoyang, Henan, China. Her research interests include wireless sensor networks and the Internet of Things.

ZHIXIAN LI received the M.Sc. degree from the Department of Information and Control Engineering, Xi'an University of Architecture and Technology, in 2005. He is currently an Associate Professor with the School of Computer and Information Engineering, Luoyang Institute of Science and Technology, Luoyang, Henan, China. His research interests include wireless sensor networks and virtual reality augmented reality.

TIAN WANG received the B.Sc. and M.Sc. degrees in computer science from Central South University, Changsha, China, in 2004 and 2007, respectively, and the Ph.D. degree in computer science from the City University of Hong Kong, Hong Kong, in 2011. He is currently a Professor with the College of Computer Science and Technology, Huaqiao University, Xiamen, China. His research interests include wireless sensor networks, cloud computing, and fog computing.

ZHIJIAN WANG received the B.Sc. and M.Sc. degrees in computer science and the Ph.D. degree in control theory and control engineering from Central South University, in 1992, 1995, and 2007, respectively. He is currently a Professor with the Information Science School, Guangdong University of Finance and Economics, China. His research interests include system modeling, software engineering, and supply chain management.

FUQIAN JIA received the B.S. degree in the Internet of Things project from the Henan Institute of Science and Technology, in 2018, where he is currently pursuing the M.Sc. degree. His research interests include wireless sensor networks, artificial intelligence, and intelligent control.

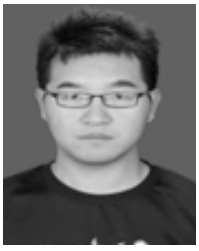

CHUNXIAO LAI received the B.S. degree in computer science and technology from Anyang Normal University, in 2013. He is currently pursuing the M.Sc. degree with the Henan Institute of Science and Technology. His research interests include wireless sensor networks and information technology.